

Effect of humidity and oxygen on friction, wear and durability of a polymer-bonded molybdenum disulfide (MoS₂)-based dry film lubricant (DFL) coating system in large amplitude fretting

E. Laolu-Balogun^a, S. Owen^b, S. Read^b, P.H. Shipway^a, K.T. Voisey^{a,*}

^a Faculty of Engineering, University of Nottingham, NG7 2RD, United Kingdom

^b Rolls-Royce Plc, Derby, United Kingdom

ARTICLE INFO

Keywords:

Dry film lubricant
Fretting
Humidity
Oxygen
Molybdenum disulphide
Environment

ABSTRACT

Investigations into effects of humidity and oxygen on a polymer-bonded MoS₂-based dry film lubricant (DFL) coating, on grit-blasted Ti–6Al–4V using a cylinder-on-flat configuration, are reported. Sustained low friction and low wear occurred in both low-humidity air and low-humidity argon, producing significant extension of fretting wear lifetimes. A cracked-paved structure was observed in low-humidity air which was not observed in low-humidity argon. The Mo-DFL coatings were observed to be highly sensitive to humidity. As humidity increased, a notable rise of friction and wear ensued which reduced the system lifetime. Different friction evolution was observed in high-humidity air and high-humidity argon before failure, with a short-lived but established low friction phase in high-humidity air and a consistent high friction phase in high-humidity argon. Although oxidation of the MoS₂ to MoO₃ is a key process of degradation of DFLs of this type, this oxidation reaction does not operate in the absence of humidity.

1. Introduction

Fretting wear is associated with the removal of material from a contact between two contacting surfaces by small oscillatory movements which can vary in frequency, amplitude and applied normal load across the contact [1,2]. This form of material degradation remains a particular problem at the dovetail joints of aero-engine fan blades, where the effects of fretting can be particularly damaging due to wide variations in the operating conditions coupled with the poor tribological properties of the titanium alloys from which such systems are commonly fabricated [3]. To curb the damaging effects of fretting of aero-engine fan blades, blades and discs are commonly surface engineered via coating, with a polymer-bonded molybdenum disulfide, MoS₂, based dry film lubricant coating as the outer layer of the coating system [4–6]. MoS₂ solid lubricants have however been reported to be highly sensitive to environmental factors such as humidity and oxygen with increases in lifetime of the coatings of more than an order of magnitude being observed [7–10]. In some work, comparisons are made between humid air and vacuum, and in these, there is ambiguity as to whether the changes in behaviour observed are associated with oxygen level, humidity level or synergy between these [10]. The issue of environmental effects on coating

performance is of particular concern given the varying atmospheric conditions in which aero-engine fan blades operate.

The detrimental effect of increased humidity on MoS₂ coatings has been attributed to water driven oxidation which causes the transformation of MoS₂ to molybdenum trioxide, MoO₃ [11–13]; it has been suggested that MoO₃ disrupts the shear properties of the MoS₂ lubricant film, causing an increase of friction coefficient and high wear rates [13–15] whilst others suggest that whilst the oxidation product MoO₃ conferred a reasonably low friction coefficient (but not as low as that conferred by MoS₂), the oxidation of MoS₂ crystals is accompanied by an increase in coating brittleness, leading to increased rates of wear [16]. As sulfur is depleted, oxygen or other elements move in to fill the vacancies and the formation of molybdenum oxide occurs which disrupts the continuity of the MoS₂ slip planes [17]. Non-oxidised, pristine, lamellae edges are thought to be relatively smooth, facilitating mutual sliding. However, after oxidation has taken place, crinkling and pitting of the edges occur which hinder lamellar movement [18,19]. Scharf et al. [20] ascribed the high friction and extremely short wear life of MoS₂ in humid air to the dangling unsaturated bonds on the edge of the basal planes reacting with moisture and oxygen in the environment to form tribo-oxidation products such as MoO₃. Bai et al. [21] also

* Corresponding author.

E-mail address: katy.voisey@nottingham.ac.uk (K.T. Voisey).

<https://doi.org/10.1016/j.wear.2024.205426>

Received 8 February 2024; Received in revised form 30 April 2024; Accepted 26 May 2024

Available online 30 May 2024

0043-1648/© 2024 The Authors. Published by Elsevier B.V. This is an open access article under the CC BY license (<http://creativecommons.org/licenses/by/4.0/>).

supported the hypothesis that dangling bonds and interlayer edges on the surface of the MoS₂ film easily react with water and oxygen in air, with the generated MoO₃ hindering the interlayer slip of the MoS₂. Thus, it exhibits a high coefficient of friction, and the wear resistance drops sharply in humid environments. However, these hypotheses need to be considered in light of the work of Windom et al. [22] who, through Raman spectroscopic studies, showed that humidity does not play a role in the oxidation of MoS₂ as no effect or transformation to MoO₃ was realised in the presence of water vapour as compared to dry air or O₂ under ambient conditions. Lince et al. [23] however found the reduction in MoS₂ coating endurance to correlate with oxidation of lubricating MoS₂ to non-lubricating MoO₃ at the surface of the coatings through XPS line scans across wear tracks of MoS₂ based sputtered coatings that had been stored in humid air. This supported the idea that the reduction in endurance is likely due to third body effects, specifically the flow of non-lubricating MoO₃ wear debris back into the contact region during testing.

This proposed mechanism of water-mediated oxidation of MoS₂ has been disputed in other studies and different mechanisms have been proposed; these are more related to the physical bonding of water to the edge sites, and thereby, disruption of easy lamellae shear of MoS₂, and therefore modification of the easy shear between the basal planes [24–26]. By investigating rubbed MoS₂ films in dry argon, dry air and moist air, Fusaro [27] found that friction coefficient and wear rates were the highest in moist air, suggesting that water causes the reduction of MoS₂ lubricity. Longer wear life, lower wear rates and lower coefficient of friction were observed in argon and dry air and higher wear rate, lower wear life and increased coefficient of friction were seen in moist air.

Pritchard and Midgley [28] investigated the friction characteristics of unbonded MoS₂ powder that was deposited on to the surface as a slurry. The resultant, adherent, polymer free surface film was approximately 1.25 mm thick. They tested this under different humidities and concluded that the friction is governed by the amount of water physically adsorbed onto the film. Indications that the water is physically adsorbed included the fact that the wear rate of the lubricant layer increased as more water is adsorbed, the reversible effects of humidity on the friction and the friction coefficient being a monotonic function of the volume of adsorbed water which was consistent with physical adsorption rather than chemical adsorption. It was thought that the water vapour affects the adhesion component of friction and therefore the inter-crystallite forces.

Khare et al. [26,29] aimed to understand the role of water, oxygen and temperature on tribological behaviour of a sputtered MoS₂ coating on 440C stainless steel. Sliding tests were performed in dry nitrogen (<300 ppm), humid nitrogen (24 % RH), dry air (<300 ppm), and humid air (60 % RH) at a range of temperatures (25–250 °C). It was found that water did not promote MoS₂ oxidation at room temperature as the Energy Dispersive X-ray Spectroscopy (EDS) results were unable to detect any oxidation following sliding in the humid environment devoid of oxygen. This study concluded that water drives the increased friction coefficients through reversible physical-sorption below transitional temperature of 100 °C by physically bonding to the near surface and directly impeding inter-lamellar shear. Increasing the temperature from ambient to the transition temperature improved the tribological response of the coating [26] in high humidity conditions. At high temperatures above 300 °C, oxygen drives increased friction due to direct oxidation which can result in a rapid deterioration of tribological properties of MoS₂ to MoO₃ [30,31].

Zhao et al. [32] proposed a model to explain the tribological behaviour and instantaneous influence of humidity on magnetron sputtered MoS₂ on stainless steel during reciprocating sliding tests with a ball-on-disk configuration at varying humidity levels from 10 to 70 % and under different atmospheric (inert and active) environments. Results showed increased humidity to be the driving force for an increased friction coefficient in all atmospheric environment including air, oxygen

and nitrogen. It was suggested that water molecules are adsorbed on the active sites and dissociate into hydroxyl groups which exhibit a strong interaction with the counter-surface. The friction coefficient was thought to be largely dependent upon the adsorbed water which was determined by the environmental humidity level; as humidity increases, more water molecules are adsorbed onto the surface and dissociate into hydroxyl groups and the attraction from hydrogen bonds becomes stronger. In active atmospheres such as oxygen, more oxides are formed which provided additional active sites for water adsorption and further increase in the observed coefficient of friction.

Upadhyay et al. [33] studied the tribological properties of epoxy/MoS₂/graphene as a function of relative humidity (40 %, 60 % and 80 %). There was an increase in the coefficient of friction and wear rates of the binary epoxy/MoS₂ composites as humidity increased. The effects of humidity were proposed to affect both the behaviour of the epoxy polymer base and the behaviour of the dispersed MoS₂ particles themselves. Adsorbed layers of water and the presence of hydroxyl groups on the polymer surface increases the adhesion forces and thereby increases the friction coefficient and the wear rate of the epoxy binder. A reaction of the MoS₂ with water molecules also produces trioxides of molybdenum, which was proposed to restrict the lubrication ability of MoS₂. It was recommended that the use of MoS₂ in epoxy should be controlled to avoid the formation of molybdenum oxides in humid environments.

The combination of physical adsorption of water and oxygen followed by a chemical reaction and the formation of molybdenum oxides have also been suggested to be the driving influence in the tribological deterioration of MoS₂ [34]. The study of surface contamination of molybdenum disulfide by Johnston et al. [35] suggested that MoS₂ which has been exposed to damp air will contain, in addition to physically adsorbed water, sulfuric acid, molybdenum trioxide, and chemisorbed water as surface contaminants.

As can be seen in this overview of the literature, there are a wide range of hypotheses which describe the mechanisms by which humidity and oxygen negatively the friction reduction capabilities and durability of molybdenum disulfide coatings; however, the behaviour and underlying mechanisms will depend upon the tribological conditions, the specific nature of the MoS₂ and the and the test or service environment. Accordingly, additional insights are required into the influential role atmospheric environmental factors have on the frictional and wear behaviours of MoS₂ coatings and particularly, on polymer bonded MoS₂ based dry film lubricant, DFL, coatings under conditions that are representative of their application in aerospace dovetail joints.

2. Experimental methodology

A cylinder-on-flat fretting contact configuration was employed as indicated in Fig. 1 where the intention is to generate reciprocating translation of the cylinder (with no rotation) across the surface of the flat sample under an applied load. This resulted in a contact length (w) of 10 mm (determined by the width of the flat sample) with the cylindrical sample having a radius, R , of 15 mm. Fretting tests were conducted with samples fabricated from Ti-6Al-4V to represent the material comprising the fan blade and disc in an aero-engine dovetail joint. Accordingly, both cylindrical and flat samples for the fretting pairs were machined from rolled plate which is reported to have an elastic modulus of 115 GPa and a Poisson's ratio of 0.342 [36] and were grit-blasted with aluminium oxide grit (Airblast, UK) with a grit size of 0.125–0.149 mm and a blast pressure of 3 bar in a manual grit-blast cabinet which resulted in a roughness (S_a) of 0.9 μm . Surface characterisation and profilometry was obtained by focus variation microscopy using an Alicona G4 Infinite Focus system. A defined area of 710 \times 539 μm was measured for determination of the surface roughness (S_a) which were calculated in accordance with ISO 25178 using a cut-off wavelength of 250 μm for S-L filters.

Following surface preparation, a DFL paint was spray deposited on the working surfaces of both the cylindrical and flat fretting samples to

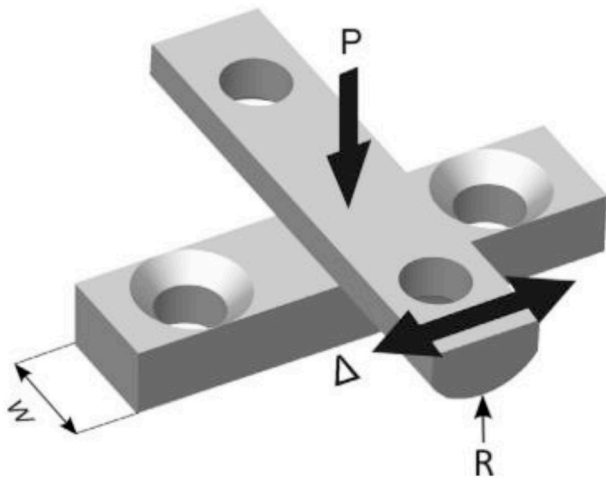


Fig. 1. Cylinder-on-flat specimen configuration used in fretting tests where P is the applied normal load, and Δ is the applied displacement.

provide alignment with industrial practice. The DFL was a commercially available epoxy-based paint (procured from Indestructible Paints Ltd, Birmingham, UK under the trade name PL237-R2), in which the primary solid lubricant phase is MoS_2 . This coating system is termed Mo-DFL from hereon. To cure the Mo-DFL coated specimens, they were placed in a circulatory air oven at $100\text{ }^\circ\text{C}$, with the temperature then being increased by $6\text{ }^\circ\text{C min}^{-1}$ to $190 \pm 1\text{ }^\circ\text{C}$ followed by holding at this temperature for 2 h. Once removed from the oven and cooled to room temperature, the target Mo-DFL coating thickness (t) of $50 \pm 10\text{ }\mu\text{m}$ coating thickness was confirmed via an eddy current method using a DeFelsko PosiTector 6000. The MoS_2 particle size in the DFL has been measured at $2\text{--}4\text{ }\mu\text{m}$ through examination of high magnification SEM images.

Fretting wear tests were carried out using a servo-hydraulic fretting testing machine; a schematic diagram of the test setup is presented in Fig. 2. As described by Aldham et al. [37], the rig employs spherical bearing seats with a seat locking system to facilitate alignment of the line contact employed. In this arrangement, two pairs of identical specimens are fretted simultaneously on the same fixture; this

arrangement ensures no damaging lateral load is carried by the hydraulic actuator whilst also facilitating an efficient replication of test contacts exposed to a given set of conditions. A linear variable displacement transducer (LVDT) is mounted to the base of the hydraulic actuator to provide the control signal for the applied (far-field) displacement amplitude (Δ^*) whilst a load cell measures the total shear force (i.e., the sum of that associated with the two individual fretting contacts, Q). The fretting test conditions were selected in light of the work of Kim and Korsunsky [38] where it was indicated that these are representative of those experienced by aerospace components where DFLs of this type are employed; in addition, these conditions allow direct comparison with other work conducted at the University of Nottingham on these DFLs [36,39,40]. A summary of the fretting test parameters and conditions are presented in Table 1.

The control and data acquisition system used an NI USB 6000 multifunction I/O device along with a written program in LAB-VIEW™ which permitted real time monitoring and continuously recorded the tangential force and applied relative displacement at 500 Hz sampling rate garnering 200 sampling points per fretting cycle. An assumption was made that the tangential force associated with each of the two fretting contacts was equal, and therefore the tangential force on each specimen was assumed to be a half of the total tangential force measured by the load cell. The tangential force-displacement data were plotted in the commonly-employed form of fretting loops of the type presented in Fig. 3 (see Ref. [41] for further details). The coefficient of friction (CoF) (μ) is given by:

$$\mu = \frac{Q^*}{P} \quad (1)$$

where Q^* is the maximum tangential force per specimen recorded in each cycle and P is the constant normal load applied. The slip amplitude (δ^*) observed at the contact itself is smaller than the applied (far-field) displacement amplitude (Δ^*) as there is compliance in the system,

Table 1
Fretting test conditions employed.

Normal Load (P)/N	575
Displacement amplitude Δ^* / μm	300
Frequency (f)/Hz	2.5

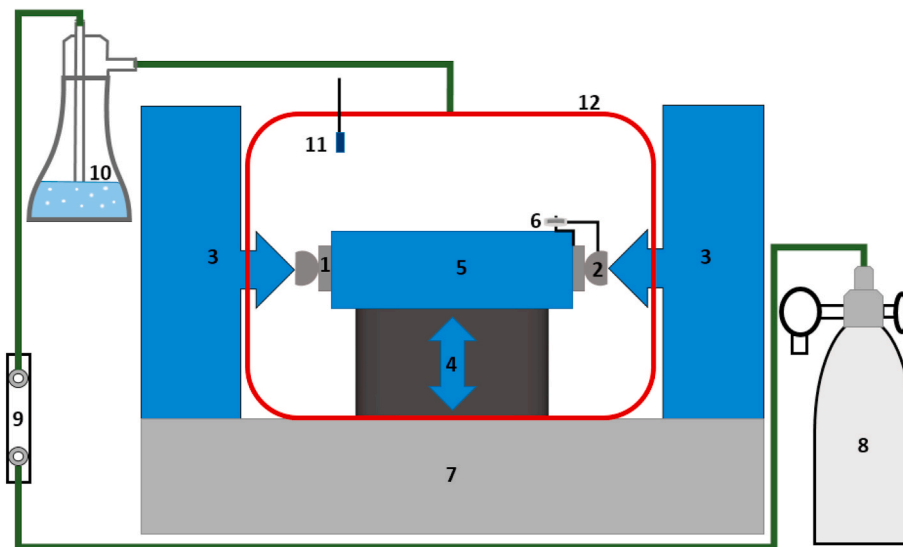


Fig. 2. Electro servo hydraulic fretting rig operating schematics and environmental set up (1) Ti–6Al–4V flat specimen with contact length $w = 10\text{ mm}$ (2) Ti–6Al–4V cylindrical specimen with radius $R = 15\text{ mm}$ (3) Fixed position hydraulic cylinder for applied normal load $P = 575\text{ N}$ (4) Vertical controlled actuator for applied displacement amplitude $\Delta^* = 0.3\text{ mm}$ (5) Load cell (6) LVDT (7) Mounting block (8) Dry air or argon cylinder (9) Flow meter (10) Water bubbler (11) Humidity sensor (12) Environment chamber.

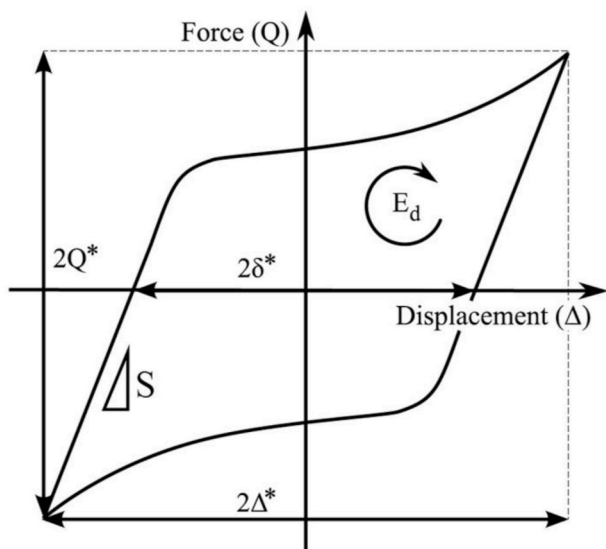


Fig. 3. Annotated schematic diagram of fretting loop (from Ref. [42]).

associated with elastic deformation of the specimen, the fixture and the test rig as indicated by the system stiffness S in Fig. 3. Previous work looking at the behaviour of DFLs with this test geometry had shown that the CoF increased rapidly towards the end of the test and that this was associated with the failure of the coating system [36]. In light of that work, failure of a test pair in the current work was defined to have occurred when $\mu \geq 0.7$ and for each material pairing type examined, tests to failure (i.e., to completion) were automatically terminated when that condition was first satisfied.

It is known that alongside the coefficient of friction itself, geometrical evolution of the contact also affects the maximum force recorded in a fretting cycle [42]. Accordingly, in this work, the energy coefficient of friction (ECoF) (μ_E) [43] has been derived in post-test analysis of the data as follows:

$$\mu_E = \frac{E_d}{4 P \delta^*} \quad (2)$$

where E_d is the energy dissipated over a fretting loop and δ^* is the slip amplitude (as distinct from the applied displacement amplitude, Δ^*).

Once the number of cycles to failure of the various fretting pairing types had been determined, interrupted tests (i.e., tests which were stopped before failure took place) were conducted on selected sample pairing types from the test matrix. Such tests were conducted to facilitate a better understanding of the wear process in the various stages of fretting degradation of these systems by permitting examination of the samples prior to final failure.

Fretting wear tests were first conducted in atmospheric ambient conditions and were then repeated in different controlled environmental conditions made possible by outfitting the fretting wear rig with environment control capabilities as illustrated in the fretting rig schematic Fig. 2. This was implemented with dry compressed air and argon gas cylinders which were purged into a purpose-built sealed environment chamber at a constant flow rate of 2 L/min to maintain a consistent gas environment. A Honeywell HIH-4000 series humidity sensor was used for the duration of the tests to measure the relative humidity inside the chamber. The NI USB 6000 and written LAB-VIEW™ program was also used for the humidity data acquisition and meant the simultaneous acquisition of the fretting wear rig data and the humidity data occurred. During selected tests, the constant flow gas purge was switched off and the environment chamber was opened to monitor the effects of the increased relative humidity during ongoing fretting tests. Further examinations on the effect of humidity required the identification of the

dominant environmental mechanism that affects the wear behaviour of the coating, and thus, it was needed to isolate the effects of oxygen and that of humidity on the performance and wear behaviour of the Mo-DFL coating. In order to test the influence of water vapour without the presence of oxygen, humidified argon was employed by passing dry argon gas at 2 L/min through a water bubbler to increase its humidity before directing it into the environment chamber. This achieved a humidity level of around 60–75 % inside the chamber. This was repeated for dry air to obtain an oxygen-containing high humidity environment. A summary of the environmental fretting test conditions can be seen in Table 2.

Additional 3D measurements (also with the Alicona system) were employed in this work to carry out surface profilometry of the wear scars from the flat and cylindrical specimens after fretting tests. These data from the Alicona system were processed using MountainsMap™. Before analysing the cylinder samples, the cylindrical surface form was first removed. From these measurements, average depth profiles across the scars were derived by taking the average of 50 individual profile lines across a scar. The key damage parameter used in this paper is the maximum wear depth derived in this way from the surface profilometry; this parameter is employed (rather than other commonly used measures of wear) since the critical issue here is the penetration (total removal) of the coating which can be most readily seen by comparing the depth of wear with the coating thickness. Where the depth of maximum wear is presented, data for the flat and cylindrical specimens are presented separately.

After fretting tests, scanning electron microscopy (SEM) was utilised for the analysis of the wear scar features, using an FEI Quanta600 MLA SEM operating with an accelerating voltage of 20 kV. Wear scars were examined both in plan-view and in cross-section; metallographic cross-sections were prepared by cold-mounting to ensure that potential degradation of the DFL that might have been associated with hot-mounting was avoided. Whole scar SEM cross-sections are presented with different magnifications in the horizontal and vertical directions to allow the characteristic features of the scars to be better presented to the reader; however, it is noted that this leads to image distortion of which the reader needs to be aware. Energy dispersive X-ray (EDX) analysis was performed in the SEM for quantitative chemical characterisation of the various features of the fretting wear scars. The EDX results are based on multiple measurements, with representative results being reported.

The BSE cross-sections presented in Fig. 4 confirm that the as deposited DFL was approximately 50 μm thick. This is clearly seen in both cross-sections in the regions adjacent to, but outside of, the wear scar. The cross-sections also show the uniformity of the distribution of MoS₂ throughout the layer and the low surface roughness of the exterior surface, Sa < 0.1 μm .

The cross-sections also confirm that the Mo-DFL coatings tested here are behaving in line with the three stage lifetime previously observed by the authors [36,39,40]. This prior work used a combination of cross-sectional SEM micrographs, profilometry results and fretting results to demonstrate that for the vast majority of the coating lifetime, stages I & II, the wear depth is within the coating. It is only in stage III when the significant increase in ECoF is seen, that wear penetrates beyond the coating into the underlying material. The main, useful, lifetime of the DFL is stage II. In the current work, wear depths were simply measured in order to be able to correlate the progress of wear

Table 2
Environment fretting test conditions.

Environment conditions	Relative Humidity (%)	Temperature (T)/°C
Dry Argon	0.5–3 ± 3	30 ± 5
Humidified argon	60–75 ± 3	30 ± 5
Dry air	0.5–3 ± 3	30 ± 5
Ambient air	25–40 ± 3	25 ± 5
Humidified air	60–75 ± 3	30 ± 5

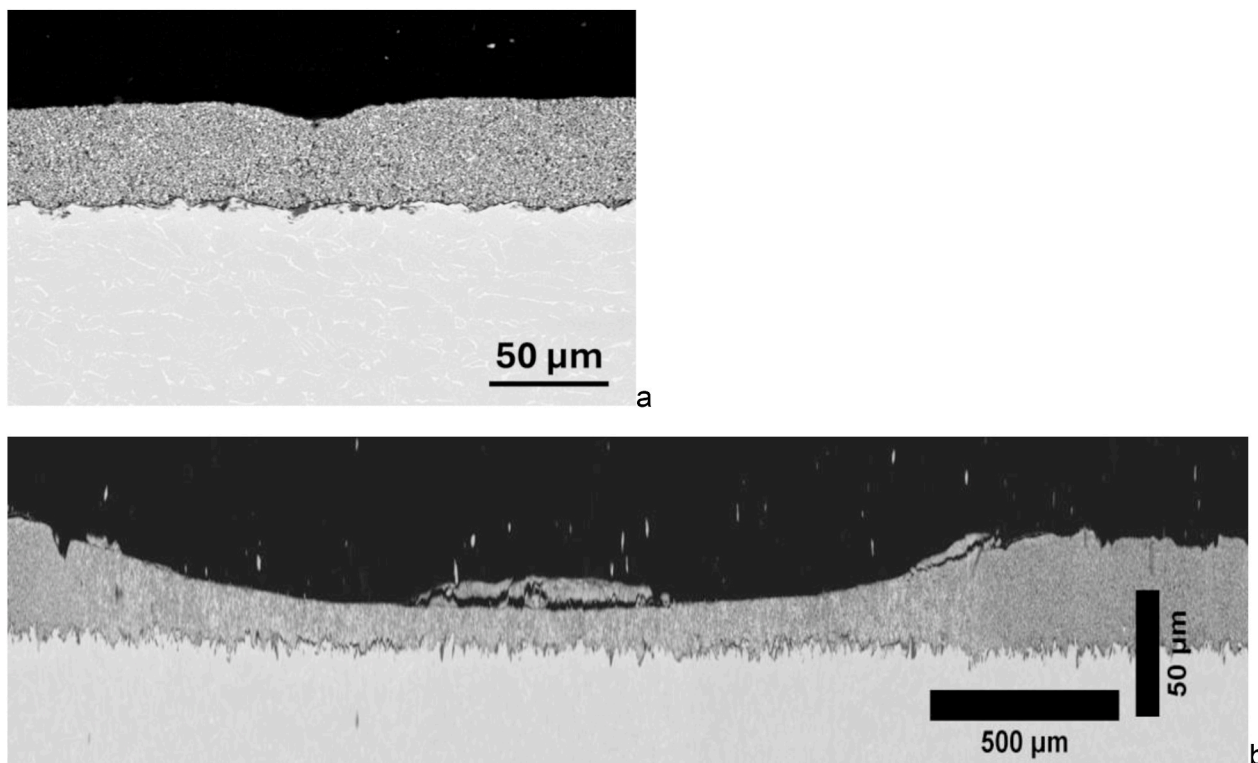


Fig. 4. BSE images of specimen cross sections, in each case the sliding direction is horizontal. a. Mo-DFL low humidity argon sample after 600 kcycles. b whole scar image for Mo-DFL high humidity argon sample interrupted after 27 kcycles, note the different scales used in x and y directions.

with these previously established lifetime stages. Such wear depths were measured for both the flat and round counter body.

3. Results

3.1. Friction evolution and coating degradation in low-humidity conditions

Fig. 5a shows the evolution of ECoF against test duration for tests conducted in the various environments. In atmospheric conditions (air with ambient humidity of $\sim 30\%$), failure was reached at ~ 65 k cycles; the three distinct stages of wear behaviour as outlined in previous work [36,39,40] were again observed where the beginning of the test (Stage I) featured an initial period of high friction followed by a low friction phase (Stage II) which lasts for approximately 40 k cycles and subsequently leads to failure phase of the coating (Stage III) which is characterised by instability and the increase of friction until the imposed limit ($\mu \geq 0.7$) was reached.

To investigate behaviour in Stage II, the test conducted in low-humidity air was deliberately stopped at 600 k cycles, before failure was reached. The test conducted in a low-humidity, oxygen-free environment (dry argon gas purge) was similarly stopped at 600 k cycles, before failure occurred. In the low-humidity conditions (with or without oxygen), a low stable friction dominated the test exposure where an ECoF of ~ 0.13 was maintained until the tests were stopped (this is much lower than ECoF at any stage in the test conducted in air with ambient humidity). In Fig. 5b, wear depths taken from averaged wear profiles on the flat and cylindrical specimens are shown; upon failure at ~ 65 k cycles, the test conducted in ambient atmosphere has worn to depths of $>50\ \mu\text{m}$ on both the flat and round specimen, indicating that the full thickness of the DFL had been removed (this being $50 \pm 10\ \mu\text{m}$). In low-humidity conditions, the flat and cylindrical samples have worn to depths of $<15\ \mu\text{m}$ in both air and argon environments, despite the test exposures being more than nine times longer than that of the test

conducted in ambient atmosphere; the small wear depths indicate that the DFL layer has not been penetrated during the test.

Plan-view BSE SEM images of the flat wear surface tested in low-humidity air (stopped at 600 k cycles) are shown in Fig. 6 where a cracked-paved structure is present on the wear surface. EDX point analysis of this surface details a high composition of Mo ($\sim 42.5\ \text{wt}\%$), S ($\sim 17.2\ \text{wt}\%$) as well as a high oxygen content of $\sim 40\ \text{wt}\%$ with no titanium detected.

Plan-view BSE SEM images of the flat specimen wear surface tested in low-humidity argon (and stopped at 600 k cycles) are shown in Fig. 7. Here, a very different surface appearance is evident; the cracked-paved structure seen after testing in low-humidity air condition was absent. EDX point analysis (Fig. 7b) indicated a relatively low oxygen content of $12.5\ \text{wt}\%$ on the wear surface with high Mo ($48.3\ \text{wt}\%$) and S ($38.8\ \text{wt}\%$) content and again no evidence of titanium. It is assumed that the oxygen detected was due to reaction of the surface following testing when the samples were brought into an air atmosphere.

Results shown in Fig. 8 detail traces of the evolution of friction against cycles alongside the recorded relative humidity for fretting tests that were conducted in low-humidity air conditions and stopped at both 300 k and 600 k cycles to assess the wear evolution of Mo-DFL coating system in low-humidity conditions and gain additional insight into the influence of humidity on the wear performance. Here, a steady-state low friction is maintained until the point of interruption. A further test was conducted where which was stopped at 815 k cycles; the dry air gas purge was maintained until 720 k cycles but then turned off whereupon the humidity increased slowly due to air exchange with the laboratory atmosphere driven by the movement of the servo-hydraulic ram. As the humidity increased from 0.5 to $6.7\ \%$ (at a rate of approximately $0.6\ \%$ per hour), a rise in ECoF from 0.1 to 0.15 was observed. As is highlighted in the enlarged section of the graph included in Fig. 8a, there is a lag of approximately 20 k cycles, 2 h 12 min, between the measured humidity starting to increase and the observed increase in ECoF. During this time lag, the humidity had risen to about $1.7\ \%$. It is thus proposed that this is

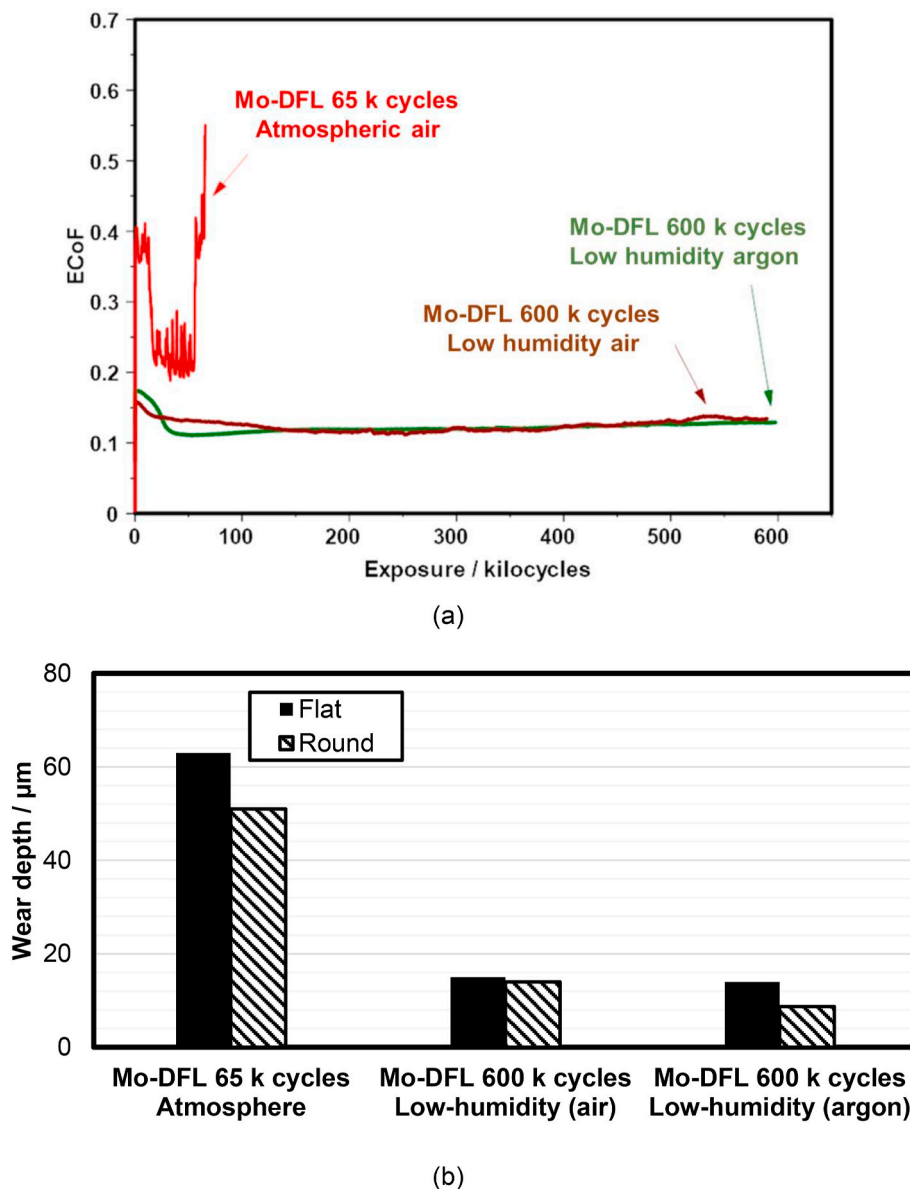


Fig. 5. Performance of the as-received MoS_2 bonded DFL coating (Mo-DFL) in tested ambient ($\sim 30\%$ RH) air and in low humidity air and argon. (a) ECoF evolution against test exposure of self-mated grit-blasted Mo-DFL coating system in different atmospheric conditions (b) The maximum depths of the averaged wear profiles taken from the wear surface upon failure for the Mo-DFL upon failure at 65 k cycles in atmospheric air and at 600 k cycles upon test interruption in different atmospheric conditions.

a maximum humidity below which the low friction-low wear state can be maintained.

In Fig. 8b, wear depths of the corresponding tests are presented, it shows that the low-humidity tests that were stopped at 300 k cycle and 600 k had very similar wear depths of between 12 and 15 μm on both the flat and cylindrical specimens. In the test where the humidity had been allowed to rise, it is noted that ECoF began to rise after 765 k cycles and that the test was terminated at 815 k cycles (before failure was deemed to have taken place). Thus, it ran for only 50 k cycles at the end of the test with the elevated ECoF and yet the observed wear depths were much larger, being ~ 19 and 29 μm on the flat and cylindrical specimens respectively. In Fig. 9, plan-view BSE SEM images of the flat specimens from the three tests are presented. Here, a cracked paved-like structure is present in all these surfaces tested in low-humidity air (with oxygen), irrespective of duration; however, the surface following the extended tests with rising humidity shows much more surface damage (with coarser features) than the surfaces seen following the other two tests.

In light of these observations, a test was conducted where the first 416 k cycles were performed in low humidity air (dry air gas purge), whereupon the gas purge was turned off and the humidity was rapidly raised to that of ambient laboratory air ($\sim 38\%$) by opening the environmental chamber to the air. As can be seen in Fig. 10, a sharp rise in relative humidity occurred (blue line) which directly correlated with a sharp rise in friction coefficient from 0.1 to 0.38 (orange line). It is also noted that upon the exposure of the surface which had been tested in low humidity condition to the higher ambient humidity ($\sim 38\%$), the ensuing fretting wear behaviour closely emulates the wear behaviour of a sample which had been tested in that ambient environment from the start (also included as the red line in Fig. 10 for comparison). Specifically, it is noted that the three wear stages are observed in both tests once they are exposed to humid air. For the sample initially tested for 416 k cycles in dry air and then exposed to humid air, failure occurred after 483 k cycles. The period in humid air was therefore 67 k cycles, and it is noted that this was very similar to the failure lifetime of the sample

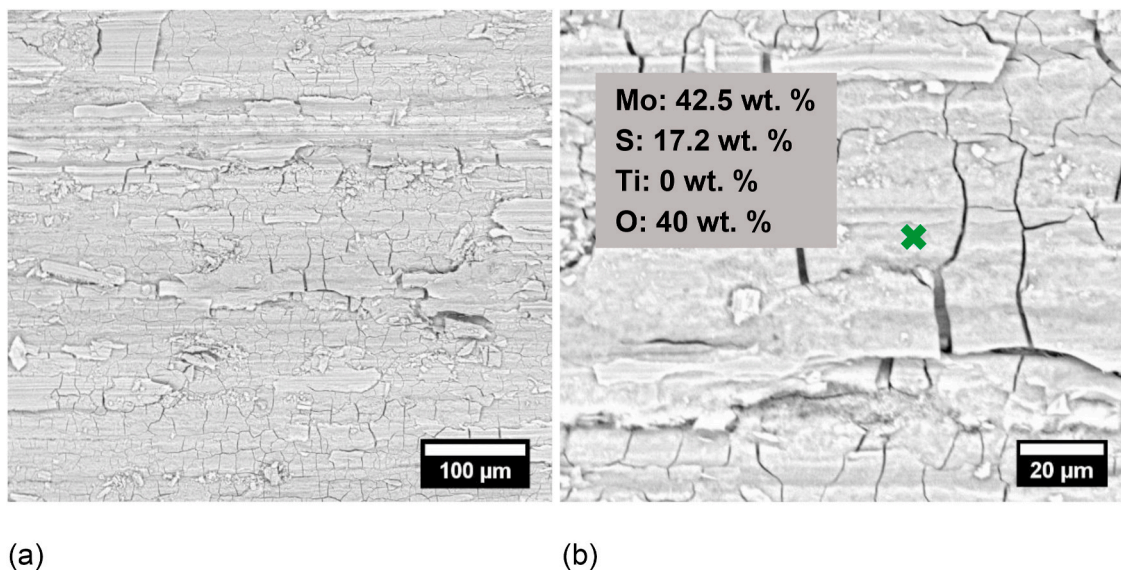


Fig. 6. Plan-view BSE SEM images of the flat specimen of the Mo-DFL coating in low-humidity air conditions which was interrupted at 600 k cycles, sliding direction was horizontal with respect to orientation of the images (a) Low magnification image (b) High magnification image with EDX point analysis.

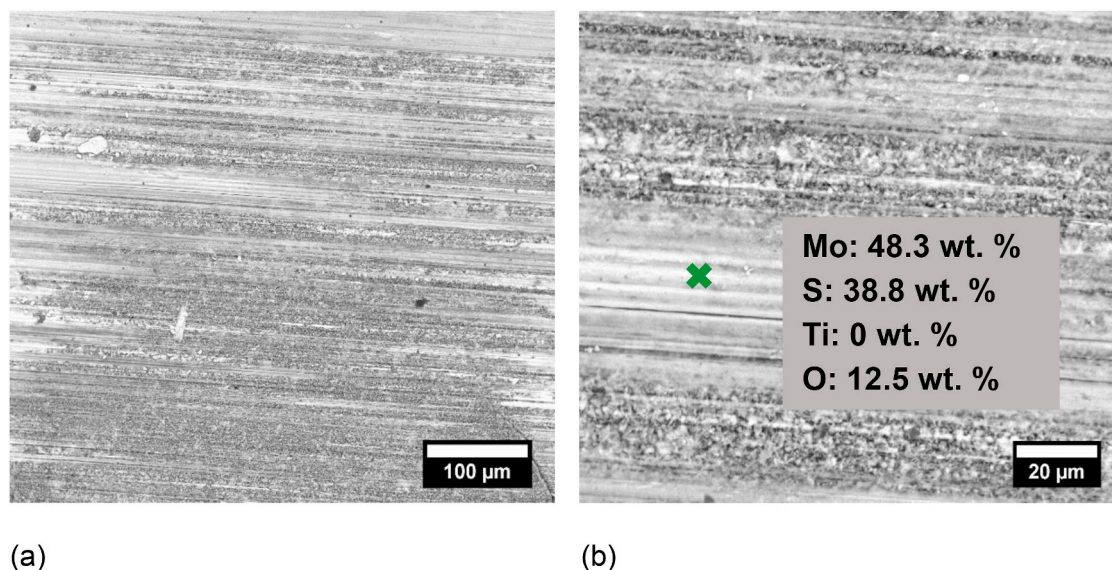


Fig. 7. Plan-view BSE SEM images of the flat specimen of the Mo-DFL coating in low humidity argon conditions which was interrupted at 600 k cycles, sliding direction was horizontal with respect to orientation of the images (a) Low magnification image (b) High magnification image with EDX point analysis.

tested in humid air alone (65 k cycles), suggesting that the damage incurred by the DFL during fretting in very low humidity was almost negligible.

3.2. Friction evolution and coating degradation in high-humidity conditions

Fretting wear behaviour in atmospheric, low-humidity air and low-humidity argon conditions have been shown in Fig. 5 where the water content in the environment can be seen to have considerable effects on the friction and wear durability of the polymer-bonded MoS₂-based DFL (Mo-DFL) coated fretting system. To gain additional insight into how the increase of humidity in the surrounding environment further influences the wear behaviour of the Mo-DFL fretting system, tests were conducted with increased humidity levels of 60–75 %. Increased humidity conditions in both oxygen-containing and oxygen-free environments were established by passing the compressed dry air or dry argon gas flow

through a water bubbler system before directing the mixture into the rig environmental chamber. In Fig. 11, the evolution of ECoF in fretting tests in ambient laboratory air and in high humidity air and argon are presented. In ambient atmosphere (~25–40 % RH), a fretting lifetime of 65 k cycles was observed before failure ($\mu \geq 0.7$). As noted previously, the three distinct stages of wear were observed in this system [36,39,40] whereby, stages; I, II and III are ascribed to the initial high friction phase followed by a low friction period and finally rising friction to failure.

By increasing the humidity levels to 60–75 % in air, similar fretting wear behaviour was observed, with the three stages again being observed, but with a reduced lifetime of 44 k cycles (Fig. 11). Most notably, the low friction phase (Stage II) when ECoF drops to ~ 0.25 exhibits a considerably shorter duration of only ~ 8 k cycles compared to the 40 k cycles observed in ambient atmospheric conditions. A very different evolution of ECoF is observed in high humidity (60–75 % RH) argon with the low friction steady state phase (Stage II) previously observed in ambient atmosphere and high humidity air being absent. In

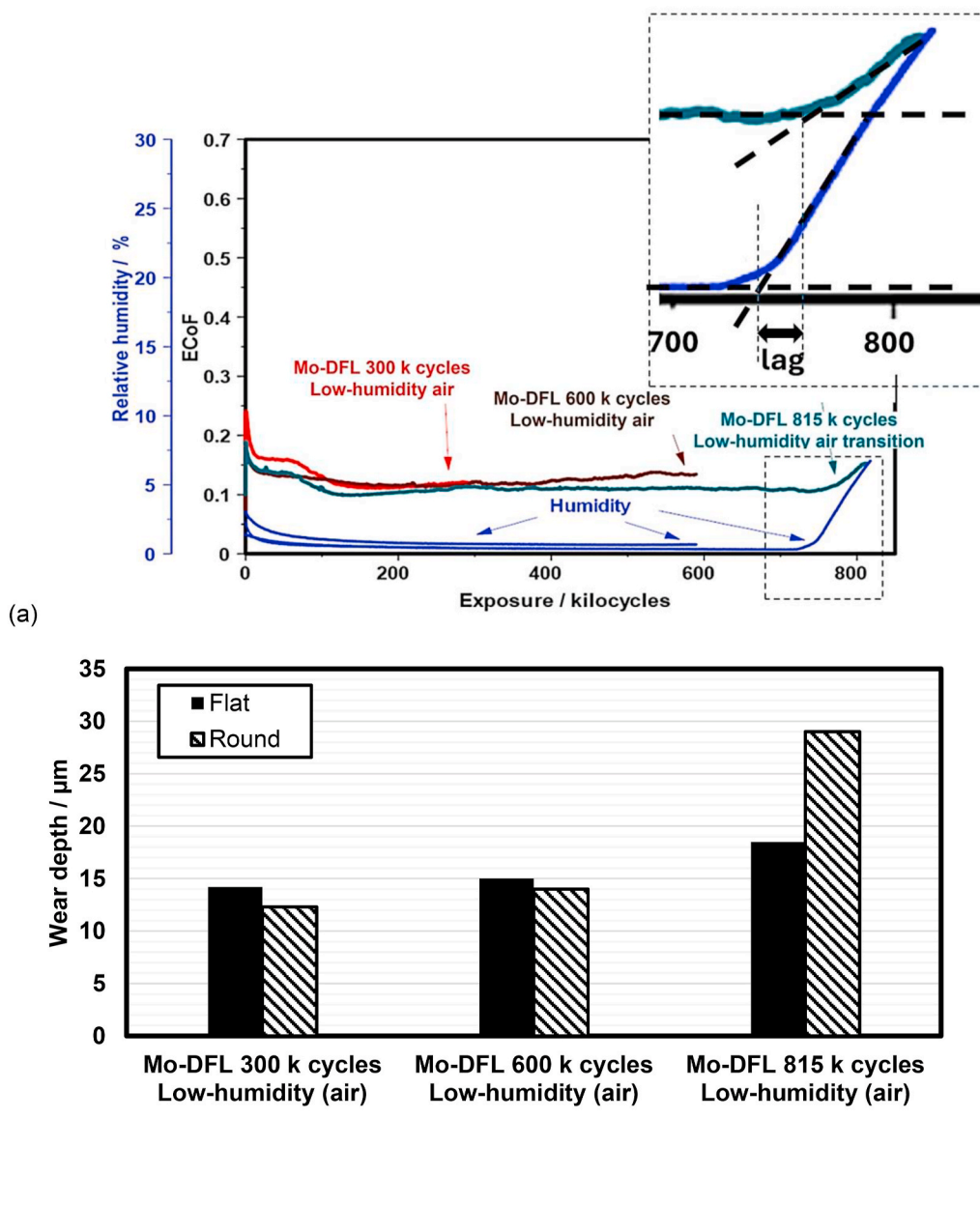


Fig. 8. Performance of the as-received MoS₂ bonded DFL coating (Mo-DFL) which were interrupted and failure had not occurred at test duration intervals of 300 k cycles, 600 k cycles in low-humidity air and at 815 k cycles at low humidity to atmospheric air transition. (a) Friction evolution against cycles of fretting tests of self-mated grit-blasted Mo-DFL coating system in low-humidity air at 300 k cycles, 600 k cycles and 815 k cycles (in low-humidity to atmospheric transition) (b) The maximum depths of the averaged wear profiles taken from the wear surface upon interruption at 300 k cycles, 600 k cycles in low-humidity air and at 815 k cycles in low humidity to atmospheric humidity transition.

this test, an initial increase of friction from ~ 0.24 to ~ 0.43 takes place which is then maintained for the majority of the fretting test until failure is reached at 54 k cycles.

To examine the development of wear occurring in ambient atmospheric air and high-humidity argon environments, additional tests, as shown in Fig. 12a, were conducted which were interrupted before the failure; specifically, these were interrupted at 23 k cycles (during the low-friction Stage II phase) in the test in ambient air and at 27 k cycles in the test in high-humidity argon when ECoF was 0.4. Wear depths (taken from the averaged wear profiles) of the resulting flat and cylindrical wear samples following interruption can be observed in Fig. 12b. In all cases, the wear depths were greater than 40 μm , with the wear on the cylinder in the ambient air test being just about 50 μm . These depths indicate that the majority of the ~ 50 μm thick DFL had been penetrated

by the time the tests were interrupted, despite the interruption point being around a third and a half of the total lifetime for the ambient atmosphere test and high humidity argon test respectively.

In Fig. 13, plan-view BSE SEM images of the flat specimens tested in atmospheric air (Fig. 13a and b) and high-humidity argon (Fig. 13c and d) which were stopped before their failure point (at 23 k cycles and 27 k cycles respectively) are shown. The micrographs along with the EDX point analyses show different phases on the wear surfaces on both of the tests. There are regions rich in Mo and S (indicating that the DFL remains here) and rich in titanium from the underlying alloy substrate, indicating that the DFL has been removed in places. A high oxygen content was found to be present in all cases. Perhaps most notably, the cracked-paved like appearance of the worn surfaces observed in the low humidity conditions (see Fig. 6) is not observed here at all, indicating a

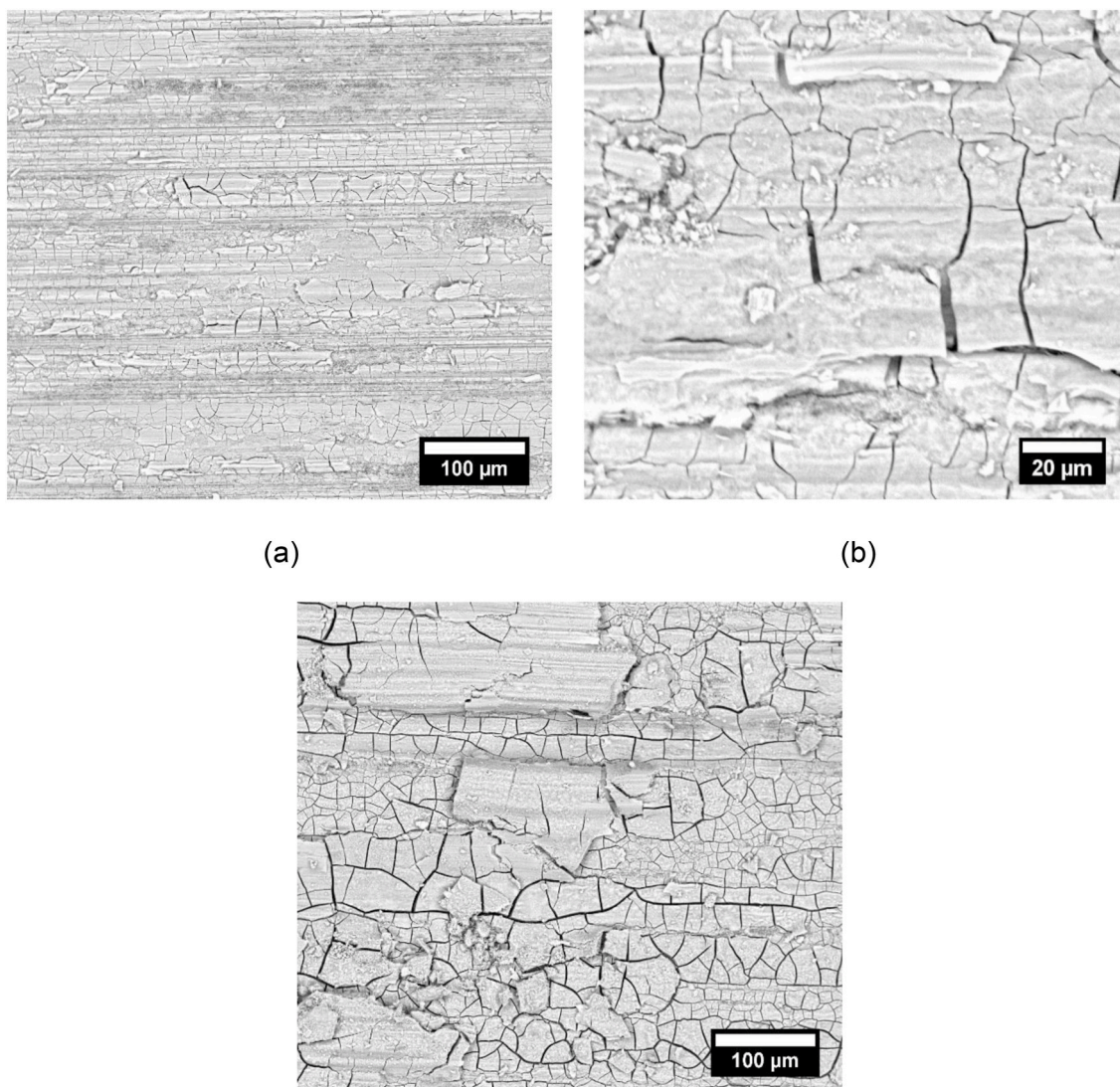


Fig. 9. Plan-view BSE SEM images of flat specimen of Mo-DFL low-humidity air tests interrupted at various test duration intervals, sliding direction was horizontal with respect to orientation of the images. (a) 300 k cycles (b) 600 k cycles (c) 815 k cycles which was terminated after a period of continuously increasing humidity had been imposed.

different mechanism of material degradation operates in the two cases.

4. Discussion

The evolution of friction of Mo-DFL in low-humidity conditions (0.5–3 % RH) and system durability as observed in Fig. 5a indicate that very different wear mechanisms operate when compared to ambient atmospheric air conditions (25–40 % RH). A steady state low friction phase was maintained at an ECoF \sim 0.13 in low-humidity conditions (in both air and argon environments) until the tests were deliberately stopped at 600 k cycles. In ambient atmospheric air (–5–40 % RH), a dynamic wear behaviour was initiated whereby three distinct wear stages of MoS₂ wear [17,39] occurred before the coating failed at 65 k cycles. These results are in accord with those observed in literature with the majority of studies maintaining the narrative that MoS₂ has low friction and low wear characteristics in low-humidity conditions [7,8,11].

The driving wear mechanism that spurs this humidity-dependent behaviour of MoS₂ however remains a point of contention in literature

where two main mechanisms have been proposed [8]. This includes the tribo-oxidative degradation of the MoS₂ to MoO₃ in a moist environment as a product of oxidation to disrupt the shear properties of the MoS₂ lubricant film, causing an increase of friction coefficient and high wear rates [13–15,44]. This disrupts the basal layer during sliding and limits the effectiveness and lifetime of MoS₂ as a solid lubricant [23,22]. The second proposed mechanism is physisorption which entails the adsorption and physical bonding of water molecules to the edge sites which increases the adhesion forces between the sliding interfaces and disrupts the easy lamellar shear [28,29,35]. In this work, the effects of oxygen in low-humidity conditions have been observed to be marginal in regards to the influence of friction, wear durability and lifetime of the Mo-DFL coating. As shown in Fig. 5a, a steady state low friction and low wear phase is preserved for the duration of the tests (before the tests were deliberately stopped at 600 k cycles) in low-humidity air and in low-humidity argon environments. The low friction and low wear capabilities of Mo-DFL are evident irrespective of the oxygen content in the environment. This leads to the conclusion that it is the water content in the environment and not the oxygen which is the driving factor behind

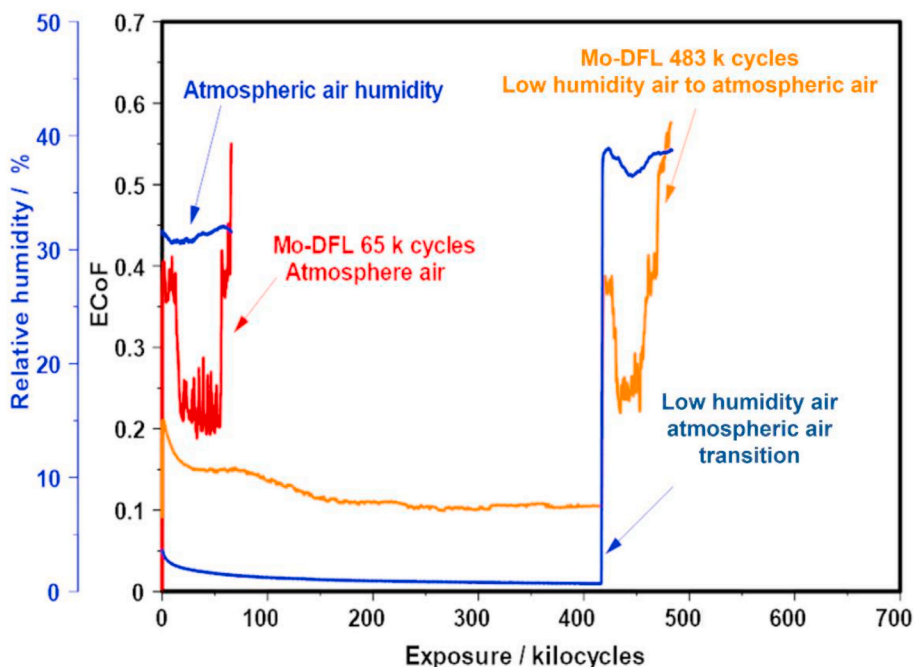


Fig. 10. Friction evolution against cycles showing fretting tests of self-mated grit-blasted Mo-DFL coating tests in atmospheric air conditions and a test initially conducted in low-humidity air and transitioned to atmospheric air condition.

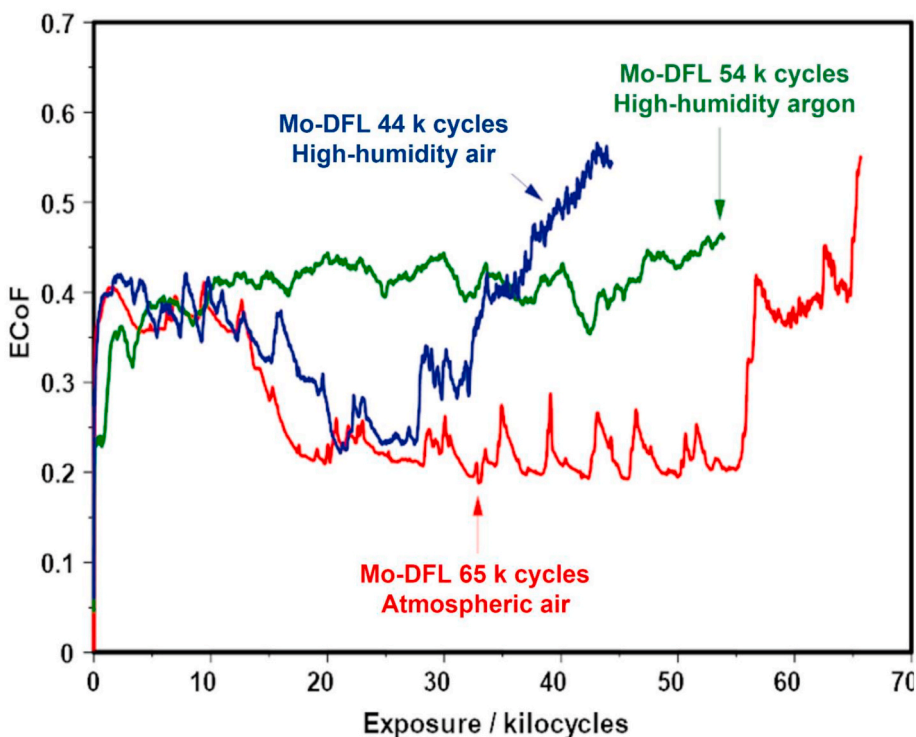


Fig. 11. Friction evolution against cycles showing fretting tests of self-mated grit-blasted Mo-DFL coating in atmospheric air, high-humidity air and high-humidity argon conditions.

the friction and wear behaviours of the MoS₂-based lubricant coating which is in agreement with previous studies [27,26,45].

Although oxygen has been shown not to affect the low friction and low wear capabilities of the Mo-DFL coating system in low-humidity conditions (Fig. 5), it is clear that oxygen does have an effect on the wear surface chemistry and subsequently, the tribo-oxidative mechanism as seen when analysing the plan-view BSE-SEM images of the flat

wear specimen tested in low-humidity air environment (Fig. 6) which shows a cracked-paved structure at the surface interface. On the surface of the test conducted in low-humidity argon (Fig. 7), the cracked-paved structure was absent. The gravimetric ratio of Mo:S in MoS₂ is 1.5:1. After testing in dry argon, the ratio at the surface is 1.25:1 whereas after testing in dry oxygen, it is 2.47:1. This increased ratio of Mo:S along with the high oxygen content (Fig. 6b) suggests that the surface is composed

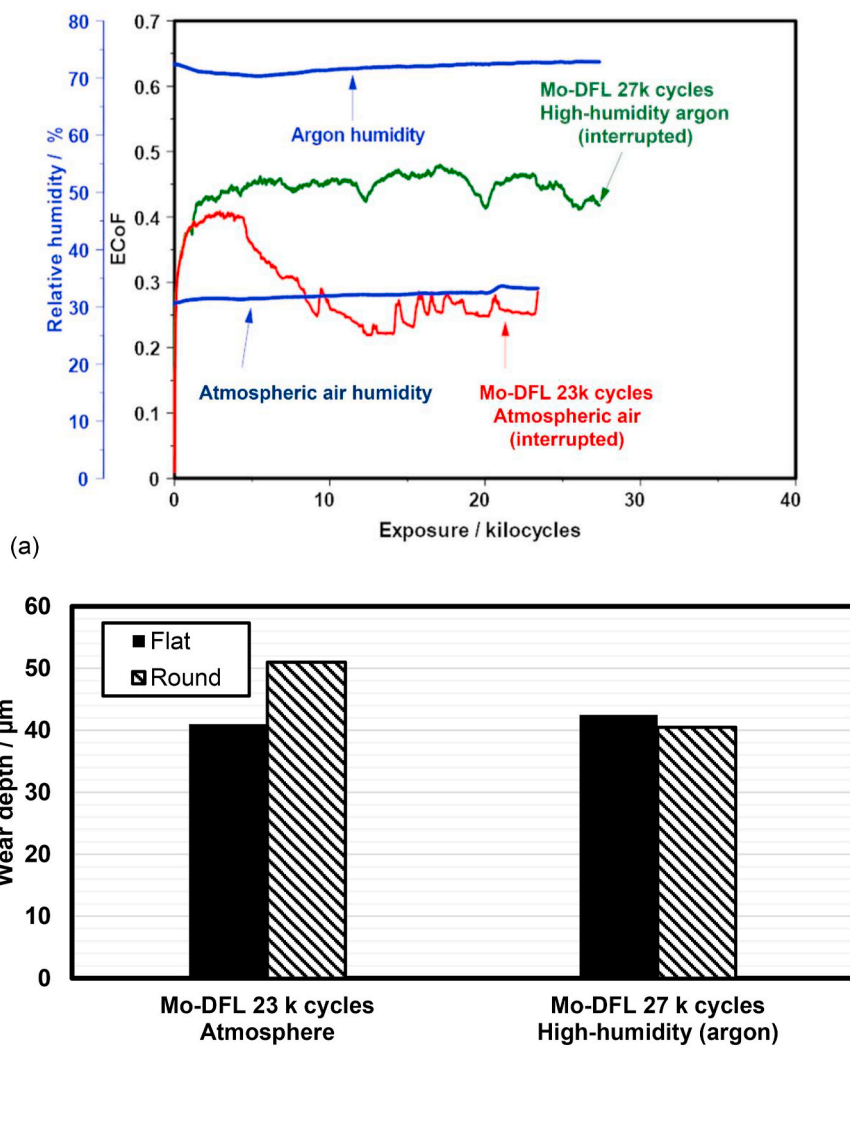


Fig. 12. (a) Interrupted friction evolution against cycles of fretting tests of self-mated grit-blasted Mo-DFL coating in atmospheric air which was stopped at 23 k cycles and high-humidity argon environment stopped at 27 k cycles before the point (b) Wear depths of corresponding interrupted tests.

of molybdenum oxide when tested in dry air, which indicates that whilst the extended low friction and low wear characteristics of Mo-DFL are not affected by oxygen in low humidity conditions, different tribo-chemical interactions are apparent.

Further evidence of the sensitivity of Mo-DFL to moisture is presented in Fig. 8a where fretting tests conducted in low-humidity air conditions until the point of interruption at testing durations of 300 k cycles and 600 k cycles maintain a steady state low friction phase (ECoF ~ 0.13) and low wear depths $<15 \mu\text{m}$ (Fig. 8b). Low-humidity air conditions were maintained until 720 k cycles whereupon the dry air gas purge into the environmental chamber was stopped and the humidity increased from 0.5 to 6.7 % (at a rate of approximately 0.6 %/hour). ECoF was observed to also rise from 0.1 to 0.15 and the wear depth had increased to ~ 19 and $29 \mu\text{m}$ on the flat and cylindrical specimens respectively upon interruption at 815 k cycles. An additional test was conducted where the first 416 k cycles were performed in low-humidity air with the environment then being changed to ambient laboratory air (~ 38 %) by opening the environmental chamber to the air as seen in Fig. 10. This resulted in a rapid rise of ECoF from 0.1 to 0.38 with the following progress of friction and wear closely following that in a fretting test that had only been conducted in an ambient atmospheric air

environment (Fig. 10), approximately 67 k cycles after the low-humidity air test was exposed to the ambient air which is also a similar lifetime to a test solely conducted in ambient atmospheric air which failed at 65 k cycles. This indicates that, prior to ambient air exposure, limited damage had occurred on the Mo-DFL coating system and it is only after air with increased humidity was introduced to the system that the progression of fretting wear damage resumes.

The demonstrated sensitivity and the observed behaviours of the Mo-DFL in low and high humidity conditions (with and without the presence of oxygen) suggests a water driven physisorption as proposed in previous studies [26,32,35,46], is likely to be a driving factor which causes increased friction, increased wear and degradation of the polymer-bonded MoS₂-based DFL coating and not an effect of oxygen.

As observed in Fig. 11, further increasing the humidity from ambient atmospheric air (25–40 % RH) to high-humidity air (~ 75 % RH) led to further reduction in the overall fretting lifetimes from 65 k cycles to 44 k cycles respectively. Although, similar fretting wear behaviours were still maintained, the increase of humidity led to a shorter duration of the low friction (Stage II [40]) phase (~ 8 k cycles) when compared to the extended low friction duration of ~ 40 k cycles observed in ambient atmospheric air. This suggests that increasing humidity in the Mo-DFL

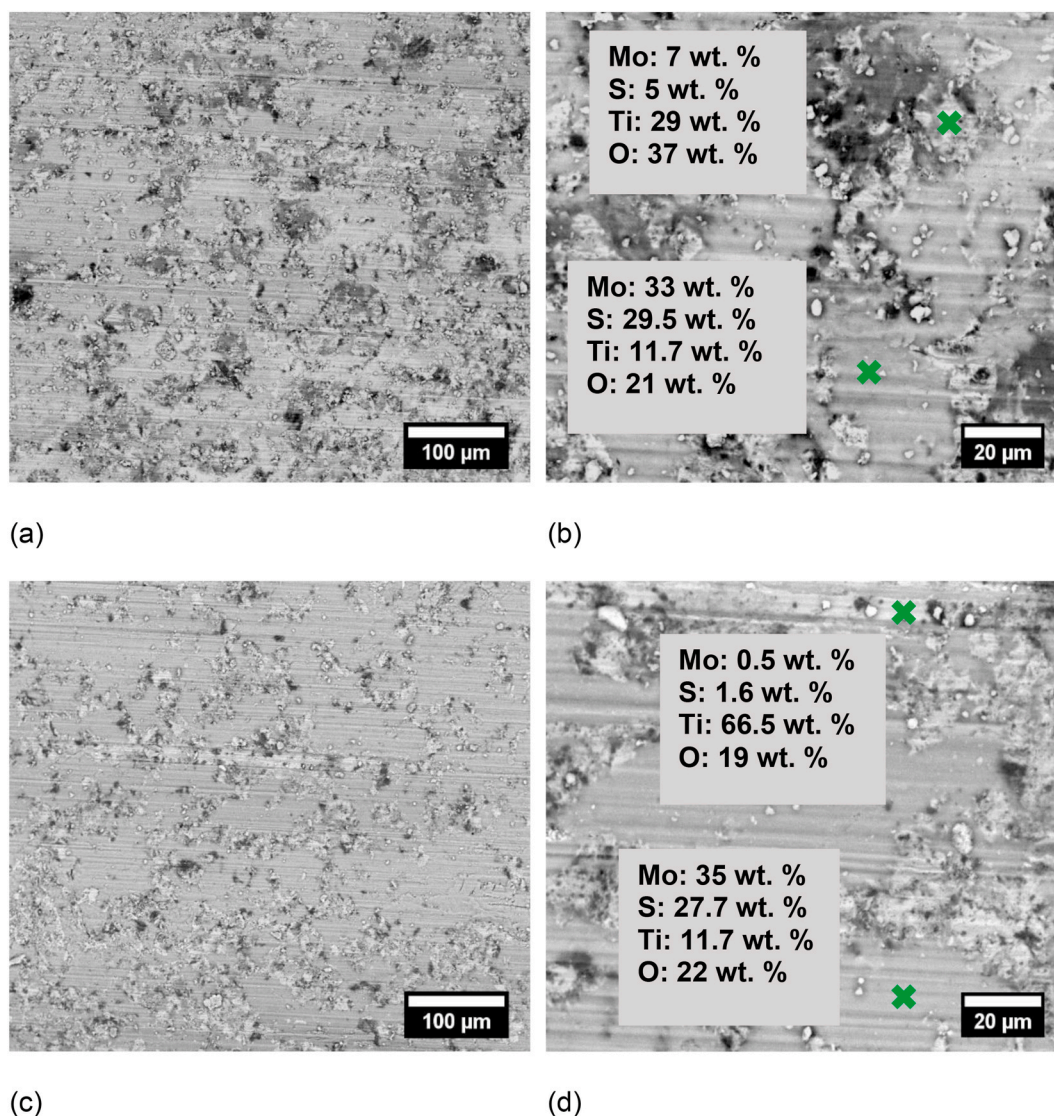


Fig. 13. Plan-view BSE SEM images of flat specimen of interrupted Mo-DFL tests, sliding direction was horizontal with respect to orientation of the images. (a) Low magnification of interrupted atmospheric air test (b) high magnification and EDX point analysis of interrupted atmospheric air test stopped at 23 k cycles. (c) Low magnification of interrupted high-humidity argon test (d) High magnification and EDX point analysis on interrupted high-humidity argon test stopped at 27 k cycles.

coating system further limits the overall lifetime and the maintenance of a low friction phase.

In high-humidity argon environment a different wear mechanism was perceived to be active where the low friction phase (Stage II) was absent from the evolution of friction as was observed in the ambient and high humidity air (Fig. 11). To chart the friction evolution and the physical wear evolution of the Mo-DFL coating occurring at the contacting surfaces during the fretting wear tests, interrupted tests before failure were conducted in ambient atmospheric air conditions which was stopped during the low friction phase (Stage II) at 23 k cycles (at an ECoF \sim 0.25), and, in high-humidity argon environment which was stopped at 27 k cycles (at an ECoF \sim 0.4) as shown in Fig. 12a.

Diverging paths of the evolution of friction in atmosphere air and high-humidity argon conditions can be observed as well as the comparable wear depths presented in Fig. 12b which suggests similar progression of wear was occurring in the two different environments, despite the differences in evolution of friction traces shown (Fig. 12). Further evidence of the comparable wear evolution is presented through plan-view SEM micrographs of the interrupted flat specimens of tests conducted in atmospheric air (terminated at 23 k cycles) shown in Fig. 13a and b and in high-humidity argon (terminated at 27 k cycles)

shown in Fig. 13c and d. Regions of molybdenum and titanium were observed at the wear interfaces (as confirmed by EDX point analysis) on both fretting wear scars indicates that although differing evolutions of friction are active in the two different environments, the physical wear process of the Mo-DFL coating in both environments are comparable. It is also noted that inhomogeneous wear scar surfaces are a feature of both the specimen tested in atmospheric air and in high-humidity argon (Fig. 13). This is evident from both the contrast in the BSE images and the EDX results, and is quite different to the comparatively featureless wear scar surfaces seen for the low humidity tests (Fig. 7). However, the differences in evolution of friction (in particular, the absence of Stage II in the test conducted in argon) indicate that oxygen plays a role in enabling the low friction phase (Stage II) within the wear process of the polymer-bonded MoS₂-based coating system in higher humidity environments; however, the mechanism behind this difference remains unclear at the present time.

In this work, different types of Mo-DFL low friction behaviours have been identified. Firstly, an extended, steady state low friction ($< \sim 0.15$) is exhibited in low-humidity conditions (0.5–3 % RH) which is active throughout the thickness of the bulk DFL coating thickness (Fig. 8) which generates a cracked-paved oxygen-rich interface in air (oxygen

containing) environment (Fig. 6); however, it is also observed in oxygen-free dry environments, although the oxygen-rich interface is not observed in this case. The second type of low friction behaviour ($> \sim 0.2$) is observed only when the Mo-DFL was worn so that the surfaces in contact are made up of a mixture of Mo-DFL and titanium (Stage II [40]); this type of low friction behaviour is only observed in air conditions (i.e. not in argon) as observed in Figs. 12a and 13a & b.

5. Conclusion

In this study, the effects of humidity and oxygen on the tribological performance of a polymer-bonded MoS₂ based DFL coating system (Mo-DFL) were examined to better understand the mechanisms that drive fretting wear behaviours in oxygen-rich (air) and oxygen free (argon) environments at both low and high humidity. The following conclusions could be made:

- The Mo-DFL coating was observed to be highly sensitive to the water content in the surrounding atmosphere. With the exposure to ambient atmosphere (humid air), the wear progression follows three distinct wear stages; a rapid increase of ECoF, followed by a short-lived low friction phase which is different to the low friction phase experienced in low-humidity conditions before the onset of coating failure.
- In low-humidity air, (0.5–3 % RH), a steady-state low friction and low wear phase is active and maintained for the entire fretting duration until tests were stopped at 600 kcycles (this interruption already being approximately x10 the lifetime attained in ambient humid air).
- Minimal damage was incurred on the ~ 50 μm thick DFL during fretting in very low humidity conditions (both oxygen-rich (air) and oxygen-free (argon)) even with an extended test period of 600 k cycles.
- Whilst oxygen was observed to not significantly affect the low friction and low wear capabilities in low-humidity conditions, a cracked-paved surface is formed on the Mo-DFL coating in low-humidity air but not in low-humidity argon. Lower oxygen content was recorded on the surface sample of tests conducted in low-humidity argon environment which suggests different tribo-chemical interactions occur at the interface.
- In atmospheric and high-humidity conditions, oxygen appears to contribute to the formation of a low friction phase (Stage II) within the evolution of friction of Mo-DFL.

CRedit authorship contribution statement

E. Laolu-Balogun: Writing – original draft, Methodology, Investigation, Formal analysis. **S. Owen:** Supervision, Conceptualization. **S. Read:** Supervision. **P.H. Shipway:** Writing – review & editing, Writing – original draft, Supervision, Methodology, Investigation, Conceptualization. **K.T. Voisey:** Writing – review & editing, Writing – original draft, Supervision.

Declaration of competing interest

The authors declare that they have no known competing financial interests or personal relationships that could have appeared to influence the work reported in this paper.

Data availability

The authors are unable or have chosen not to specify which data has been used.

Acknowledgements

The work presented in this paper formed part of Emmanuel Laolu-Balogun's PhD which was funded by an EPSRC industrial CASE award run with Rolls Royce plc.

References

- [1] D.B. Luo, V. Fridrici, P. Kapsa, Relationships between the fretting wear behavior and the ball cratering resistance of solid lubricant coatings, *Surf. Coating. Technol.* 204 (8) (2010) 1259–1269.
- [2] R.B. Waterhouse, P.H. Shipway, Fretting wear, in: *Fretting Wear*, 2007.
- [3] D.S. Wei, Y.R. Wang, Analysis of fretting fatigue life of dovetail assemblies based on fracture mechanics method, *Eng. Fail. Anal.* 25 (2012) 144–155.
- [4] D.B. Luo, V. Fridrici, P. Kapsa, Selecting solid lubricant coatings under fretting conditions, *Wear* 268 (5–6) (2010) 816–827.
- [5] J. Xu, M. Zhu, Z. Zhou, P. Kapsa, L. Vincent, An investigation on fretting wear life of bonded MoS₂ solid lubricant coatings in complex conditions, *Wear* 255 (1–6) (Aug. 2003) 253–258.
- [6] Y. Ye, J. Chen, H. Zhou, An investigation of friction and wear performances of bonded molybdenum disulfide solid film lubricants in fretting conditions, *Wear* 266 (7–8) (2009) 859–864.
- [7] W.O. Winer, Molybdenum disulfide as a lubricant: a review of the fundamental knowledge, *Wear* 10 (1967) 422–452.
- [8] Z. Chen, X. He, C. Xiao, S.H. Kim, Effect of humidity on friction and Wear-A critical review, *Lubricants* 6 (3) (2018).
- [9] X. Zhao, S.S. Perry, The role of water in modifying friction within MoS₂ sliding interfaces, *ACS Appl. Mater. Interfaces* 2 (5) (2010) 1444–1448.
- [10] N. Hiraoka, Wear life mechanism of journal bearings with bonded MoS₂ film lubricants in air and vacuum, *Wear* 249 (2001) 1014–1020.
- [11] J.K. Lancaster, A review of the influence of environmental humidity and water on friction, lubrication and wear, *Tribol. Int.* 23 (6) (Dec. 1990) 371–389.
- [12] A.J. Haltner, C.S. Oliver, Effect of water vapor on friction of molybdenum disulfide, *Ind. Eng. Chem. Fundam.* 5 (3) (1966) 348–355.
- [13] J.K.G. Panitz, L.E. Pope, J.E. Lyons, D.J. Staley, Tribological properties of MoS₂ Coatings in vacuum, low relative humidity and high relative humidity environments 1166 (June 1998) (1987) 2–7.
- [14] S. Ross, A. Sussman, Surface oxidation of molybdenum disulfide, *J. Phys. Chem.* 59 (9) (1955) 889–892.
- [15] K.S. Randhawa, A. Patel, The Effect of Environmental Humidity/water Absorption on Tribo-Mechanical Performance of Polymers and Polymer Composites – a Review, *Ind. Lubr. Tribol.*, May, 2021.
- [16] J. Yin, H. Yan, M. Cai, S. Song, X. Fan, M. Zhu, Bonded flake MoS₂ solid lubricant coating: an effective protection against fretting wear, *J. Ind. Eng. Chem.* 117 (2023) 450–460.
- [17] M.N. Gardos, The synergistic effects of graphite on the friction and wear of MoS₂ films in air, *Tribol. Trans.* 31 (2) (1988) 214–227.
- [18] A.W.B. Gwidon Stachowiak, Solid lubrication and surface treatments, in: *Engineering Tribology*, Technology, Butterworth-Heinemann, 2013, pp. 485–526.
- [19] G. Salomon, A.W.J. De Gee, J.H. Zaat, Mechano-chemical factors in MoS₂-film lubrication, *Wear* 7 (1) (Jan. 1964) 87–101.
- [20] T.W. Scharf, P.G. Kotula, S.V. Prasad, Friction and wear mechanisms in MoS₂Sb₂O₂ Au nanocomposite coatings, *Acta Mater.* 58 (12) (2010) 4100–4109.
- [21] Y. Bai, J. Pu, H. Wang, L. Wang, Q. Xue, S. Liu, High humidity and high vacuum environment performance of MoS₂/Sn composite film, *J. Alloys Compd.* 800 (2019) 107–115.
- [22] B.C. Windom, W.G. Sawyer, D.W. Hahn, A Raman spectroscopic study of MoS₂ and MoO₃: applications to tribological systems, *Tribol. Lett.* 42 (3) (2011) 301–310.
- [23] J.R. Lince, S.H. Loewenthal, C.S. Clark, Tribological and chemical effects of long term humid air exposure on sputter-deposited nanocomposite MoS₂ coatings, *Wear* 432–433 (December 2018) (2019).
- [24] J.M. Martin, C. Donnet, L. Mogne, Superlubricity of molybdenum disulfide, *Ind. Lubric. Tribol.* 52 (1) (1993) 13–18.
- [25] C. Donnet, J.M. Martin, T. Le Mogne, M. Belin, The origin of super-low friction coefficient of MoS₂ coatings in various environments, *Tribol.* 27 (C) (1994) 277–284.
- [26] H.S. Khare, D.L. Burris, The effects of environmental water and oxygen on the temperature-dependent friction of sputtered molybdenum disulfide, *Tribol. Lett.* 52 (3) (2013) 485–493.
- [27] R.L. Fusaro, Lubrication and failure mechanisms of molybdenum disulfide films. 1: effect of atmosphere, *NASA Tech. Pap.* 1343 (1978).
- [28] J.M.C. Pritchard, J.W. Midgley, The effect of humidity on the friction and life of unbonded molybdenum disulfide films, *Wear* 13 (1969) 39–50.
- [29] H.S. Khare, D.L. Burris, Surface and subsurface contributions of oxidation and moisture to room temperature friction of molybdenum disulfide, *Tribol. Lett.* 53 (1) (2014) 329–336.
- [30] F. Meng, C. Yang, H. Han, Study on tribological performances of MoS₂ coating at high temperature, *Proc. Inst. Mech. Eng. Part J J. Eng. Tribol.* 232 (8) (2018) 964–973.
- [31] H. Han, Z. Qian, F. Meng, Z. Cui, Tribological performances of graphite–MoS₂ coating at various high temperatures, *Proc. Inst. Mech. Eng. Part J J. Eng. Tribol.* 233 (12) (2019) 1888–1902.
- [32] X. Zhao, G. Zhang, L. Wang, Q. Xue, The tribological mechanism of MoS₂ film under different humidity, *Tribol. Lett.* 65 (2) (2017) 1–8.

- [33] R.K. Upadhyay, A. Kumar, Effect of humidity on the synergy of friction and wear properties in ternary epoxy-graphene-MoS₂ composites, *Carbon N. Y.* 146 (May 2019) 717–727.
- [34] W.L. Spychalski, M. Pisarek, R. Szoszkiewicz, Microscale insight into oxidation of single MoS₂ crystals in air, *J. Phys. Chem. C* 121 (46) (2017) 26027–26033.
- [35] R.R.M. Johnston, A.J.W. Moore, Water adsorption on molybdenum disulfide containing surface contaminants, *J. Phys. Chem.* 68 (11) (1964) 3399–3406.
- [36] K. Barman, P.H. Shipway, K.T. Voisey, G. Pattinson, The role of a thermally sprayed CuNiIn underlayer in the durability of a dry-film lubricant system in fretting – a phenomenological model, *Tribol. Int.* 123 (Jul. 2018) 307–315.
- [37] D. Aldham, J. Warburton, R.E. Pendlebury, The unlubricated fretting wear of mild steel in air, *Wear* 106 (1985) 177–201.
- [38] K. Kim, A.M. Korsunsky, Effects of imposed displacement and initial coating thickness on fretting behaviour of a thermally sprayed coating, *Wear* 271 (2011) 1080–1085.
- [39] E. Laolu-Balogun, S. Owen, T. Booth, G. Pattinson, P.H. Shipway, K.T. Voisey, Lifetime of MoS₂ based DFL systems in fretting with and without a Cu-Ni-In underlayer: the dependence on the topography of the surface onto which the DFL is deposited, *Tribol. Int.* 188 (2023) 108863.
- [40] K. Barman, P.H. Shipway, K.T. Voisey, G. Pattinson, Evolution of damage in MoS₂-based dry film lubricants (DFLs) in fretting wear—the effect of DFL thickness and contact geometry, *Prog. Org. Coating* 105 (2017) 67–80.
- [41] S.R. Pearson, P.H. Shipway, Is the wear coefficient dependent upon slip amplitude in fretting? Vingsbo and Söderberg revisited, *Wear* 330–331 (2015) 93–102.
- [42] X. Jin, W. Sun, P.H. Shipway, Derivation of a wear scar geometry-independent coefficient of friction from fretting loops exhibiting non-Coulomb frictional behaviour, *Tribol. Int.* 102 (2016) 561–568.
- [43] S. Fouvry, P. Duó, P. Perruchaut, A quantitative approach of Ti-6Al-4V fretting damage: friction, wear and crack nucleation, *Wear* 257 (9–10) (2004) 916–929.
- [44] T.B. Stewart, P.D. Fleischauer, Chemistry of sputtered molybdenum disulfide films, *Inorg. Chem.* 21 (6) (1982) 2426–2431.
- [45] E. Serpini, A. Rota, A. Ballestrazzi, D. Marchetto, E. Gualtieri, S. Valeri, The role of humidity and oxygen on MoS₂ thin films deposited by RF PVD magnetron sputtering, *Surf. Coating. Technol.* 319 (Jun. 2017) 345–352.
- [46] R. Holinski, J. Gänsheimer, A study of the lubricating mechanism of molybdenum disulfide, *Wear* 19 (3) (1972) 329–342.